Energy-norm a posteriori error estimates for singularly perturbed reaction-diffusion problems on anisotropic meshes. Neumann boundary conditions

Natalia Kopteva

1 Introduction

This paper addresses finite element approximations to singularly perturbed semilinear reaction-diffusion equations of the form

$$-\varepsilon^2\triangle u + f(x,y;u) = 0 \ \text{ for } (x,y)\in\Omega, \quad \partial_\nu u = \psi \text{ on } \Gamma_N, \quad u = 0 \text{ on } \Gamma_D, \qquad (1)$$

posed in a, possibly non-Lipschitz, polygonal domain $\Omega\subset\mathbb{R}^2$. Here $0<\varepsilon\leqslant 1$. The boundary segments Γ_D and Γ_N are disjoint with $\bar\Gamma_D\cup\bar\Gamma_N=\partial\Omega$, and ∂_ν denotes the outward normal derivative. The function f is continuous on $\Omega\times\mathbb{R}$ and satisfies $f(\cdot;s)\in L_\infty(\Omega)$ for all $s\in\mathbb{R}$, and the one-sided Lipschitz condition $f(x,y;v)-f(x,y;w)\geqslant C_f[v-w]$ whenever $v\geqslant w$, with some constant $C_f\geqslant 0$ such that $C_f+\varepsilon^2\geqslant 1$.

Our goal is to give residual-type a posteriori error estimates on reasonably general anisotropic meshes (such as on Fig. 1, left, and Fig. 2) in the energy norm $|\!|\!|\cdot|\!|\!|_{\varepsilon;\Omega}$. The latter is an appropriately scaled $W_2^1(\Omega)$ norm naturally associated with our problem. For any $\mathscr{D}\subseteq\Omega$, it is defined by

$$|\!|\!|v|\!|\!|_{\varepsilon;\mathscr{D}} := \left\{\varepsilon^2\|\nabla v\|^2_{2;\mathscr{D}} + \|v\|^2_{2;\mathscr{D}}\right\}^{1/2}.$$

The case of Dirichlet boundary conditions was considered in the recent article [9]. Now we extend this analysis to also allow boundary conditions of Neumann type. In this preliminary contribution, we shape our treatment of Neumann boundary conditions on anisotropic mesh elements in a simpler setting of partially structured meshes (as on Fig. 1, right). The presented approach will be applied to more general anisotropic meshes, such as addressed in [8, 9], in a forthcoming journal article.

N. Kopteva
Department of Mathematics and Statistics, University of Limerick, Limerick, Ireland
e-mail: natalia.kopteva@ul.ie

It is worth noting that our estimators in this paper, as well as in [8, 9, 10], do not involve the so-called matching functions. (The latter appear in the estimator error constants in [12, 13, 14]; they depend on the unknown error and take moderate values only when the grid is either isotropic, or, being anisotropic, is aligned correctly to the solution, while, in general, may be as large as mesh aspect ratios.)

We discretize (1) using linear finite elements. Let $S_h \subset \{v \in H^1(\Omega) \cap C(\bar{\Omega}) : v = 0 \text{ on } \Gamma_D\}$ be a piecewise-linear finite element space relative to a triangulation $\mathscr{T}$, and let the computed solution $u_h \in S_h$ satisfy

$$\varepsilon^2 \langle \nabla u_h, \nabla v_h \rangle + \langle f_h^I, v_h \rangle = \int_{\Gamma_N} \varepsilon^2 \psi v_h \quad \forall\, v_h \in S_h, \qquad f_h(\cdot) := f(\cdot; u_h). \tag{2}$$

Here $\langle \cdot, \cdot \rangle$ is the $L_2(\Omega)$ inner product, and f_h^I is the standard piecewise-linear Lagrange interpolant of f_h.

To give a flavour of our results, our first estimator reduces to

$$\begin{aligned} |\!|\!| u_h - u |\!|\!|_{\varepsilon;\Omega} \leqslant C \Big\{ & \sum_{z \in \mathscr{N}} \min\{h_z H_z,\, \varepsilon H_z^2 h_z^{-1}\} \big\| \varepsilon J \big\|^2_{\infty;\gamma_z} + \sum_{z \in \mathscr{N}} |I_z^\psi|^2 \\ & + \sum_{z \in \mathscr{N}} \big\| \min\{1, H_z \varepsilon^{-1}\} f_h^I \big\|^2_{2;\omega_z} + \big\| f_h - f_h^I \big\|^2_{2;\Omega} \Big\}^{1/2}, \end{aligned} \tag{3}$$

where C is independent of the diameters and the aspect ratios of elements in $\mathscr{T}$, and of ε. Here $\mathscr{N}$ is the set of nodes in $\mathscr{T}$, J is the standard jump in the normal derivative of u_h across an interior element edge, while $J := \partial_\nu u_h - \psi$ on Γ_N, ω_z is the patch of elements surrounding any $z \in \mathscr{N}$, γ_z is the set of edges originating at z and lying in $\omega_z \cup \Gamma_N$, $H_z = \operatorname{diam}(\omega_z)$, and $h_z \simeq H_z^{-1} |\omega_z|$. We also obtain a sharper version of (3), in which the interior-residual factors $\min\{1, H_z \varepsilon^{-1}\}$ are replaced by $\min\{1, h_z \varepsilon^{-1}\}$ and a few other terms are included (see (23) and Corollary 4.2).

The presence of Neumann boundary conditions is reflected in J computed on $\gamma_z \cap \Gamma_N$, and in additional (and, perhaps, unexpected) terms I_z^ψ:

$$|I_z^\psi|^2 \leqslant \min\{H_z, \varepsilon\} H_z \big| \operatorname{osc}(\varepsilon \psi; \gamma_z \cap \Gamma_N) \big|^2.$$

In the case of shape-regular triangulations, $\min\{h_z H_z, \varepsilon H_z^2 h_z^{-1}\} \simeq \min\{H_z, \varepsilon\} H_z$, while $\|J\|_{\infty;\gamma_z} \geqslant \frac{1}{2} \operatorname{osc}(J; \gamma_z \cap \Gamma_N) \geqslant \frac{1}{2} \operatorname{osc}(\psi; \gamma_z \cap \Gamma_N)$. Hence, in this case, $\sum |I_z^\psi|^2$ is bounded by the first sum in (3), so may be skipped. For the case $\varepsilon = 1$, this yields a version of the standard estimator [1, §2.2].

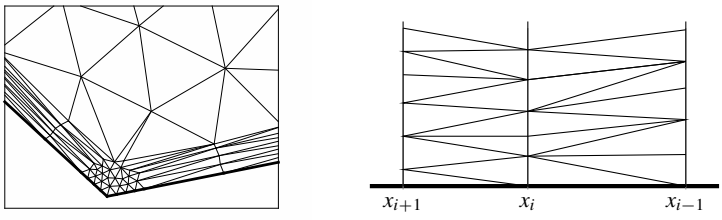

Fig. 1 Example of a mesh considered in [8, 9] (left), partially structured anisotropic mesh (right).

To relate (3) to interpolation error bounds, as well as to possible adaptive-mesh construction strategies, note that $|J_z|$ may be interpreted as approximating the diameter of ω_z under the metric induced by the squared Hessian matrix of the exact solution (while f_h^I approximates $\varepsilon^2\triangle u$).

Our interest in this paper is in general anisotropic meshes, since such meshes, when constructed a priori, have been shown to offer an efficient way of computing reliable numerical approximations of solutions that exhibit sharp boundary and interior layers (see, e.g., [2, 5, 11, 16] and references therein). In the case of shape-regular triangulations, residual-type a posteriori estimates for equations of type (1) were proved in [18] in the energy norm, and more recently in [4] in the maximum norm. The case of anisotropic meshes having a tensor-product structure was addressed in [17, 6, 3]. Above, we briefly discussed anisotropic estimators [12, 13, 14].

Note that no attempt will be made in this contribution to derive lower error bounds. For anisotropic meshes, [13] gives such a bound, which includes some of the terms appearing in our estimators. For example, in the case $h_z \leqslant \varepsilon$, the terms in first sum of (3) reduce to $h_z H_z \|\varepsilon J\|^2_{\infty;\gamma_z}$, while the related jump residual terms in the lower error bound [13, (4.2)] can can be interpreted as $\sum_{S\subset\gamma_z} h_z|S|\,\|\varepsilon J\|^2_{\infty;S}$.

The paper is organized as follows. In §2, we make basic triangulation assumptions and recall the anisotropic scaled-trace theorem from [8, 9]. The error is represented in terms of the residual in §3, while the main results are obtained in §4. We conclude the paper by presenting some numerical results in §5.

Notation. We write $a \simeq b$ when $a \lesssim b$ and $a \gtrsim b$, and $a \lesssim b$ when $a \leqslant Cb$ with a generic constant C depending on Ω and f, but C does not depend on either ε or the diameters and the aspect ratios of elements in $\mathscr{T}$. Also, for $\mathscr{D} \subset \bar{\Omega}$, $1 \leqslant p \leqslant \infty$, and $k \geqslant 0$, let $\|\cdot\|_{p;\mathscr{D}} = \|\cdot\|_{L_p(\mathscr{D})}$ and $|\cdot|_{k,p;\mathscr{D}} = |\cdot|_{W^k_p(\mathscr{D})}$, where $|\cdot|_{W^k_p(\mathscr{D})}$ is the standard Sobolev seminorm with integrability index p and smoothness index k.

2 Basic triangulation assumptions. Scaled trace bounds

We shall use $z = (x_z, y_z)$, S and T to respectively denote particular mesh nodes, edges and elements, while $\mathscr{N}$, $\mathscr{S}$ and $\mathscr{T}$ will respectively denote their sets. For each $T \in \mathscr{T}$, let H_T be the maximum edge length and $h_T := 2H_T^{-1}|T|$ be the minimum height in T. For each $z \in \mathscr{N}$, let ω_z be the patch of elements surrounding any $z \in \mathscr{N}$, $\mathscr{S}_z$ the set of edges originating at z, and

$$H_z := \operatorname{diam}(\omega_z), \quad h_z := \max_{T\subset\omega_z} h_T, \quad \gamma_z := \mathscr{S}_z\backslash\Gamma_D, \quad \mathring{\gamma}_z := \{S \subset \gamma_z : |S| \lesssim h_z\}. \quad (4)$$

Throughout the paper we make the following Triangulation Assumptions (that are automatically satisfied by shape-regular triangulations).

- *Maximum Angle condition.* Let the maximum interior angle in any triangle $T \in \mathscr{T}$ be uniformly bounded by some positive $\alpha_0 < \pi$.
- *Local Element Orientation condition.* For any $z \in \mathscr{N}$, a minimal rectangle $R_z \supset \omega_z$ is such that $|R_z| \simeq |\omega_z|$.
- Also, let the number of triangles containing any node be uniformly bounded.

Our analysis in [8, 9] applies to three node types, which we call (i) anisotropic, (ii) semi-anisotropic, and (iii) isotropic nodes (see Fig. 2). As in this preliminary contribution, only type (i) is considered, we skip the definitions (ii) and (iii).

(i) *Anisotropic Nodes*, whose set is denoted by $\mathcal{N}_{\rm ani}$, are such that

$$h_z < c_0 H_z, \qquad h_T \simeq h_z \ \text{ and } \ H_T \simeq H_z \quad \forall\, T \subset \omega_z, \tag{5}$$

where c_0 is a fixed small constant.

(i*) One typically expects anisotropic elements near Γ_D to be aligned along it. The boundary nodes for which this is not the case form a special set:

$$\mathcal{N}_D^* := \big\{\, z \in \bar\Gamma_D \cap \mathcal{N}_{\rm ani} \ : \ |\mathscr{S}_z \cap \Gamma_D| \lesssim h_z \ \text{ or } \ z \notin \bar\Gamma_N \cap \bar\Gamma_D \text{ is a corner of } \Omega \,\big\}. \tag{6}$$

Next, we recall a version of the scaled trace theorem for possibly anisotropic nodes using, with $p = 1, 2$, the scaled $W_p^1(\mathscr{D})$ norm

$$|\!|\!| v |\!|\!|_{p;\mathscr{D}} := (\operatorname{diam}\mathscr{D})^{-1} \|v\|_{p;\mathscr{D}} + \|\nabla v\|_{p;\mathscr{D}}\,.$$

In particular, in view of $\operatorname{diam}(\omega_z) = H_z$ and $\operatorname{diam}(T) \simeq H_T$,

$$|\!|\!| v |\!|\!|_{p;\omega_z} = H_z^{-1} \|v\|_{p;\omega_z} + \|\nabla v\|_{p;\omega_z}\,, \quad |\!|\!| v |\!|\!|_{p;T} \simeq H_T^{-1} \|v\|_{p;T} + \|\nabla v\|_{p;T}\,. \tag{7}$$

Lemma 2.1 (Anisotropic scaled trace bounds [8, 9]). *For any node $z \in \mathcal{N}$ of type* (5)*, and any function $v \in W_1^1(\omega_z)$, one has*

$$\|v\|_{1;\mathring\gamma_z} + \frac{h_z}{H_z}\|v\|_{1;\gamma_z\setminus\mathring\gamma_z} + \frac{h_z}{H_z}\|v\|_{1;\bar S_z} \lesssim |\!|\!| v |\!|\!|_{1;\omega_z}\,, \tag{8}$$

$$\|v\|_{1;\mathring\gamma_z} + \frac{h_z}{H_z}\|v\|_{1;\gamma_z\setminus\mathring\gamma_z} + \frac{h_z}{H_z}\|v\|_{1;\bar S_z} \lesssim \Big\{ h_z \|v\|_{2;\omega_z} |\!|\!| v |\!|\!|_{2;\omega_z} \Big\}^{1/2}, \tag{9}$$

where γ_z and $\mathring\gamma_z$ are from (4), while $\bar S_z \subset \omega_z$ is any segment that originates at z and satisfies $|\bar S_z| \simeq H_z$.

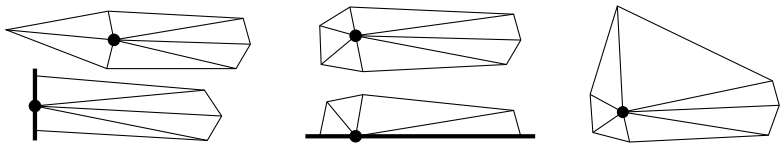

Fig. 2 Examples of anisotropic nodes $z \in \mathcal{N}_{\rm ani}$ (left), semi-anisotropic nodes $z \in \mathcal{N}_{\rm s.ani}$ (centre), an isotropic node $z \in \mathcal{N}_{\rm iso}$ (right), and a node $z \in \mathcal{N}_{\rm ani} \cap \mathcal{N}_D^*$ (bottom left); see [8, 9].

3 Representation of the error in terms of the residual

Using the monotonicity of f and $C_f + \varepsilon^2 \geqslant 1$, one gets

$$\begin{aligned}\|\!|u_h - u|\!\|^2_{\varepsilon;\Omega} &\lesssim \varepsilon^2 \langle \nabla(u_h - u), \nabla(u_h - u)\rangle + \langle f(\cdot;u_h) - f(\cdot;u), u_h - u\rangle \\ &= \varepsilon^2 \langle \nabla u_h, \nabla(u_h - u)\rangle + \langle f(\cdot;u_h), u_h - u\rangle - \int_{\Gamma_N} \varepsilon^2 \psi\,(u_h - u),\end{aligned}$$

where we also used (1). Next, assuming $\|\!|u_h - u|\!\|_{\varepsilon;\Omega} > 0$, let

$$G := \frac{u_h - u}{\|\!|u_h - u|\!\|_{\varepsilon;\Omega}} \qquad \Rightarrow \qquad \|\!|G|\!\|_{\varepsilon;\Omega} = 1. \tag{10}$$

So $\|\!|u_h - u|\!\|_{\varepsilon;\Omega} \lesssim \varepsilon^2 \langle \nabla u_h, \nabla G\rangle + \langle f(\cdot;u_h), G\rangle - \int_{\Gamma_N} \varepsilon^2 \psi G$. So (2) implies, $\forall v_h \in S_h$,

$$\|\!|u_h - u|\!\|_{\varepsilon;\Omega} \lesssim \varepsilon^2 \langle \nabla u_h, \nabla(G - v_h)\rangle + \langle f_h^I, G - v_h\rangle - \int_{\Gamma_N} \varepsilon^2 \psi\,(G - v_h) + \langle f_h - f_h^I, G\rangle. \tag{11}$$

Here $\langle f_h - f_h^I, G\rangle =: \mathscr{E}_{\text{quad}}$ is the quadrature error, for which $\|G\|_{2;\Omega} \leqslant 1$ implies

$$|\mathscr{E}_{\text{quad}}| \leqslant \|\!|f_h - f_h^I|\!\|^*_{\varepsilon;\Omega} \leqslant \|f_h - f_h^I\|_{2;\Omega}\,, \tag{12}$$

where the norm $\|\!|\cdot|\!\|^*_{\varepsilon;\Omega}$ is dual to $\|\!|\cdot|\!\|_{\varepsilon;\Omega}$; see also [9, Remark 4.1].

Next, let ϕ_z be the standard linear hat function corresponding to $z \in \mathscr{N}$, and $v_h := G_h + \sum_{z\in\mathscr{N}} \bar{g}_z \phi_z \in S_h$, where $G_h \in S_h$ is some interpolant of G, while $\bar{g}_z$ is a certain average of $G - G_h$ near z (to be specified later), but $\bar{g}_z = 0$ for $z \in \Gamma_D$ (so that $v_h \in S_h$). Now, using $g := G - G_h$, one gets $G - v_h = g - \sum_{z\in\mathscr{N}} \bar{g}_z \phi_z = \sum_{z\in\mathscr{N}} (g - \bar{g}_z)\phi_z$. Combining this with (11) gives a standard error representation

$$\begin{aligned}\|\!|u_h - u|\!\|_{\varepsilon;\Omega} &\lesssim \sum_{z\in\mathscr{N}} \varepsilon^2 \int_{\gamma_z} J(g - \bar{g}_z)\phi_z + \sum_{z\in\mathscr{N}} \int_{\omega_z} f_h^I\,(g - \bar{g}_z)\phi_z + \mathscr{E}_{\text{quad}} \\ &=: I + II + \mathscr{E}_{\text{quad}}\,,\end{aligned} \tag{13}$$

which holds for any $G_h \in S_h$ and any $\{\bar{g}_z\}_{z\in\mathscr{N}}$ such that $\bar{g}_z = 0$ whenever $z \in \Gamma_D$. Here we use a standard definition for J with $J := \partial_\nu u_h\big|_{T'} + \partial_\nu u_h\big|_{T''}$ on an interior edge $\partial T' \cap \partial T'' \neq \varnothing$ (where $T', T'' \in \mathscr{T}$), and $J := \partial_\nu u_h - \psi$ on Γ_N.

4 Error analysis for a partially structured anisotropic mesh

Our ultimate goal is to consider a reasonably general anisotropic mesh such as addressed in [8, 9] (see Fig. 1, left, and Fig. 2). But in this preliminary contribution, to illustrate our approach, we restrict the analysis to a simpler, partially structured, anisotropic mesh in a square domain. To be more precise, let

$$\Omega := (0,1)^2, \qquad \Gamma_N := \{(x,y) \in \partial\Omega : \ x = 1 \text{ or } y = 1\}, \qquad \psi(0,1) = 0. \quad (14)$$

(The condition on ψ is a compatibility condition, as $u(0,y) = 0$ implies $\partial_y u(0,1) = 0$. If it is violated, the mesh node at $(0,1)$ is expected to be isotropic, and a version of our analysis below will apply.) The following triangulation assumptions are made.

A1. Let $\{x_i\}_{i=0}^n$ be an arbitrary mesh on the interval $(0,1)$ in the x direction. Then, let each $T \in \mathcal{T}$, for some i,
   (i) have the shortest edge on the line $x = x_i$;
   (ii) have a vertex on the line $x = x_{i+1}$ or $x = x_{i-1}$ (see Fig. 1, right).

A2. Let $\mathcal{N} = \mathcal{N}_{\rm ani}$, i.e. each mesh node z satisfies (5).

A3. *Quasi-non-obtuse anisotropic elements.* Let the maximum angle in any triangle be bounded by $\frac{\pi}{2} + \alpha_1 \frac{h_T}{H_T}$ for some positive constant α_1.

These conditions essentially imply that all mesh elements are anisotropic and aligned in the x-direction. They also imply that if $x_z = x_i$, then

$$\omega_z \subseteq \omega_z^* := (x_{i-1}, x_{i+1}) \times (y_z^-, y_z^+), \quad y_z^+ - y_z^- \simeq h_z, \quad \operatorname{diam} \omega_z^* \simeq H_z, \qquad (15)$$

where (y_z^-, y_z^+) is the range of y within ω_z, and we also use $x_{-1} := x_0$ and $x_{n+1} := x_n$.

Remark 4.1. The above conditions (in particular, A3) imply that there is $J \lesssim 1$ such that $\omega_z^* \subset \omega_z^{(J)}$ for all $z \in \mathcal{N}$, with the notation $\omega_z^{(0)} := \omega_z$ and $\omega_z^{(j+1)}$ for the patch of elements in/touching $\omega_z^{(j)}$. (Note that $J = 1$ for any non-obtuse triangulation.)

4.1 Choice of $\bar g_z$. Main results

Following [8, 9], the choice of $\bar g_z$ in (13) is related to the orientation of anisotropic elements, and is crucial. Let $\bar g_z = 0$ for $z \in \Gamma_D$, and

$$\int_{x_{i-1}}^{x_{i+1}} (g(x,y_z) - \bar g_z)\, \varphi_i(x)\, dx = 0 \qquad \text{for } \ z = (x_i, y_z), \ \ 1 \leqslant i \leqslant n. \qquad (16)$$

Here we use the standard one-dimensional hat function $\varphi_i(x)$ associated with the mesh $\{x_i\}$ (i.e. it has support on (x_{i-1}, x_{i+1}), equals 1 at $x = x_i$, and is linear on (x_{i-1}, x_i) and (x_i, x_{i+1})). Note that for $z = (x_i, 0)$, in view of $g = 0$ on Γ_D, the above definition (16) agrees with $\bar g_z = 0$, earlier prescribed on Γ_D.

Remark 4.2. An inspection of standard proofs for shape-regular meshes reveals that one obstacle in extending them to anisotropic meshes lies in the application of a scaled traced theorem when estimating the jump residual terms (this causes the mesh aspect ratios to appear in the estimator). This technical difficulty is addressed by choosing $\bar g_z$ as a certain one-dimensional average of g, as in (16), or in (17) below. To relate this to standard choices, for $x_z = x_i$, let $\bar S_z \subset \omega_z^*$ be the interval joining (x_{i-1}, y_z) and (x_{i+1}, y_z), $1 \leqslant i \leqslant n$. Then (16) is identical to $\int_{\bar S_z} (g - \bar g_z)\, \varphi_i = 0$. Also, for non-obtuse triangulations, it is equivalent to $\int_{\bar S_z} (g - \bar g_z)\, \phi_z = 0$. The reader may compare this with a more standard choice, denoted here by $\bar g_z'$: $\int_{\omega_z} (g - \bar g_z')\, \phi_z = 0$ (see, e.g., [15, Lecture 5]).

Remark 4.3. It is sometimes helpful to tweak the definition (16) of $\{\bar g_z\}_{z\in\mathscr{N}}$ and use instead $\{\bar g_z^*\}_{z\in\mathscr{N}}$ defined for $z\in\mathscr{N}\setminus\Gamma_D$ with $x_z=x_i$ by

$$\int_{\omega_z^*}[g(x,y)-\bar g_z^*]\,\varphi_i(x)=0, \tag{17}$$

(where ω_z^* is from (15)), and $\bar g_z^*=0$ for $z\in\Gamma_D$. Note that

$$h_zH_z|\bar g_z^*|\lesssim\|g\|_{1;\omega_z^*},\quad H_z|\bar g_z-\bar g_z^*|\lesssim\|\nabla g\|_{1;\omega_z^*},\quad |\omega_z^*|\simeq h_zH_z. \tag{18}$$

Here the first relation is obvious, while $\int_{\omega_z^*}[g(x,y_z)-g(x,y)]\,\varphi_i(x)\simeq h_zH_z(\bar g_z-\bar g_z^*)$ implies $H_z|\bar g_z-\bar g_z^*|\lesssim\|\partial_y g\|_{1;\omega_z^*}$ and so the second relation.

Theorem 4.1 *For the solution u of* (1), (14)*, and the computed solution u_h of* (2)*, let $g=G-G_h$ with G from* (10) *and any $G_h\in S_h$, and*

$$\Theta:=\varepsilon^2\|\nabla g\|_{2;\Omega}^2+\sum_{z\in\mathscr{N}}\big(1+\varepsilon^2H_z^{-2}\big)\|g\|_{2;\omega_z}^2. \tag{19}$$

Then $|||u_h-u|||_{\varepsilon;\Omega}\lesssim I+II+\mathscr{E}_{\rm quad}$, where $\mathscr{E}_{\rm quad}$ is bounded by (12)*, and, under conditions A1–A3,*

$$|I+I^\Psi|\lesssim\Big\{\Theta\sum_{z\in\mathscr{N}}\lambda_z\big\|\varepsilon J_z\big\|_{\infty;\gamma_z}^2\Big\}^{1/2},\qquad \lambda_z:=h_zH_z\min\{1,\varepsilon H_zh_z^{-2}\}, \tag{20}$$

$$|I^\Psi|\lesssim\Big\{\Theta\sum_{\substack{z\in\mathscr{N}:\\ |\gamma_z\cap\Gamma_N|\simeq H_z}}\lambda_z'\varepsilon H_z\big|\operatorname{osc}(\varepsilon\psi;\gamma_z\cap\Gamma_N)\big|^2\Big\}^{1/2},\quad \lambda_z':=\min\{1,H_z\varepsilon^{-1}\}, \tag{21}$$

$$|II|\lesssim\Big\{\Theta\sum_{z\in\mathscr{N}}\big\|\lambda_z'f_h^I\big\|_{2;\omega_z}^2\Big\}^{1/2}. \tag{22}$$

Additionally, one has an alternative bound

$$\begin{aligned}|II|\lesssim\Big\{&\Theta\sum_{z\in\mathscr{N}\setminus\mathscr{N}_D^*}\big\|\min\{1,h_z\varepsilon^{-1}\}\,f_h^I\big\|_{2;\omega_z}^2+\Theta\sum_{z\in\mathscr{N}\setminus\mathscr{N}_D^*}\big\|\lambda_z'\operatorname{osc}(f_h^I;\omega_z)\big\|_{2;\omega_z}^2\\ &+\Theta\sum_{z\in\mathscr{N}_D^*}\big\|\lambda_z'f_h^I\big\|_{2;\omega_z}^2\Big\}^{1/2},\end{aligned} \tag{23}$$

where $\mathscr{N}_D^*=\{z\in\mathscr{N}:x_z=0\}$ (in agreement with (6)*).*

Corollary 4.2 (A posteriori error estimator) *Under the conditions of Theorem 4.1, $|||u_h-u|||_{\varepsilon;\Omega}\lesssim I+II+\mathscr{E}_{\rm quad}$, where $\mathscr{E}_{\rm quad}$ is bounded by* (12)*, while for I and II one has bounds* (20)–(23) *with $\Theta:=1$.*

Proof. Under more general conditions than A1–A3, there exists $G_h\in S_h$ such that $\Theta\lesssim|||G|||_{\varepsilon;\Omega}=1$; see [9, Theorem 7.4]. □

Remark 4.4. An inspection of the proof shows that in the bound (21) for I^ψ, one can replace $\gamma_z \cap \Gamma_N$ by $[\gamma_z \backslash \mathring{\gamma}_z] \cap \Gamma_N$, which gives a slightly sharper bound.

Proof of Theorem 4.1. We partially follow and invoke some auxiliary results from the proof of [9, Theorem 5.1]. The proof of (20) and (21) is given in §4.2 below. Note that we cannot simply focus on the new terms, denoted by I_z^N in (25), as one needs to look into a delicate interaction of a component of I_z^N and some other terms in I (see (26), (27), (29)).

For the remaining interior-residual bounds (22) and (23), an inspection of [9, Section 5.3] shows that the estimation of the interior-residual component II of the error (13) applies to our case, with the only change in that II involves $\sum_{i=1}^{n} II_i$ (rather than $\sum_{i=1}^{n-1} II_i$), where $II_i := \sum_{z \in \mathscr{N}_i} \int_{\omega_z} f_h^I(x_i, y)\,(g - \bar{g}_z^*)\,\phi_z$ is defined in [9], with $\mathscr{N}_i := \{z \in \mathscr{N} : x_z = x_i\}$, while $\mathscr{N}_{\partial\Omega}^*$ of [9] is now denoted $\mathscr{N}_D^* = \mathscr{N}_0$. Note also that (17) and (18), as well as Remark 4.5 below, are crucial for (22) and (23). □

4.2 Jump Residual. Proof of (20) and (21)

Proof of (20) and (21). Split I of (13) as $I = \sum_{z \in \mathscr{N}} I_z$, where

$$I_z := \varepsilon^2 \int_{\gamma_z} J(g - \bar{g}_z)\phi_z. \tag{24}$$

When considering J on $\gamma_z \backslash \partial\Omega = \gamma_z \backslash \Gamma_N$, we adapt the notational convention that the unit normal ν to any edge in γ_z takes the clockwise direction about z, while $[\![w]\!]$, for any w, is the jump in w across any edge in γ_z evaluated in the anticlockwise direction about z. Then

$$J\big|_{\gamma_z \backslash \Gamma_N} = [\![\nabla u_h]\!] \cdot \nu = [\![\partial_x u_h]\!] \nu_x + [\![\partial_y u_h]\!] \nu_y\,.$$

So I_z can be split as

$$\begin{aligned} I_z = I_z' + I_z'' + I_z''' + I_z^N := {} & \varepsilon^2 \int_{\gamma_z \backslash \Gamma^N} (g - \bar{g}_z)\phi_z [\![\partial_x u_h]\!]\, \nu_x + \varepsilon^2 \int_{\mathring{\gamma}_z \cap \Gamma^N} J(g - \bar{g}_z)\phi_z \\ & + \varepsilon^2 \int_{\gamma_z \backslash \Gamma^N} [g - g(x, y_z)]\, \phi_z [\![\partial_y u_h]\!]\, \nu_y \\ & + \varepsilon^2 \int_{\gamma_z \backslash \Gamma^N} [g(x, y_z) - \bar{g}_z]\, \phi_z [\![\partial_y u_h]\!]\, \nu_y \\ & + \varepsilon^2 \int_{[\gamma_z \backslash \mathring{\gamma}_z] \cap \Gamma^N} (\partial_\nu u_h - \psi)(g - \bar{g}_z)\phi_z\,. \end{aligned} \tag{25}$$

For the final term here one has, using $\partial_\nu u_h = \partial_y u_h$ on $[\gamma_z \backslash \mathring{\gamma}_z] \cap \Gamma^N \subset \partial\Omega \cap \{y = 1\}$,

$$I_z^N = \varepsilon^2 \int_{[\gamma_z \backslash \mathring{\gamma}_z] \cap \Gamma^N} \partial_y u_h (g - \bar{g}_z)\phi_z - \underbrace{\varepsilon^2 \int_{[\gamma_z \backslash \mathring{\gamma}_z] \cap \Gamma^N} \psi (g - \bar{g}_z)\phi_z}_{=: I_z^\psi}\,. \tag{26}$$

We claim that to get the desired assertions (20) and (21), it suffices to show that

$$|I'_z| + |I''_z| \lesssim \varepsilon \,|\!|\!| g |\!|\!|_{1;\omega_z^*} \left\| \varepsilon J \right\|_{\infty;\gamma_z}, \qquad I'''_z + (I_z^N + I_z^\psi) = 0, \tag{27}$$

$$|I_z| \lesssim \varepsilon \frac{H_z}{h_z} \left\{ h_z \|g\|_{2;\omega_z^*} \,|\!|\!| g |\!|\!|_{2;\omega_z^*} \right\}^{1/2} \left\| \varepsilon J \right\|_{\infty;\gamma_z}, \tag{28}$$

and

$$|I_z^\psi| \lesssim \varepsilon \left\{ H_z \|g\|_{2;\omega_z^\psi} \,|\!|\!| g |\!|\!|_{2;\omega_z^\psi} \right\}^{1/2} \mathrm{osc}(\varepsilon\psi; [\gamma_z \backslash \mathring{\gamma}_z] \cap \Gamma_N). \tag{29}$$

In (29),

$$\omega_z^\psi := (x_{i-1}, x_{i+1}) \times (1 - H_z, 1) \qquad \text{for any } \; z = (x_i, 1), \quad i = 1, \dots, n, \tag{30}$$

is an isotropic rectangle with the upper edge $[\gamma_z \backslash \mathring{\gamma}_z] \cap \Gamma_N$ (a similar triangle can be used instead).

To show that (20) and (21), indeed, follow from (27)–(30), let

$$\begin{aligned} \theta_z &:= \lambda_z^{-1} \varepsilon^2 \min\Big\{ |\!|\!| g |\!|\!|^2_{1;\omega_z^*} \,, H_z^2 h_z^{-1} \|g\|_{2;\omega_z^*} |\!|\!| g |\!|\!|_{2;\omega_z^*} \Big\}, \\ \theta_z^\psi &:= \lambda_z'^{-1} \varepsilon \|g\|_{2;\omega_z^\psi} \,|\!|\!| g |\!|\!|_{2;\omega_z^\psi} \,. \end{aligned}$$

Note that an application of $\min(a, bc)/\min(1, c) \leqslant a + b$ (for any $a, b, c > 0$) implies $\theta_z \lesssim \varepsilon^2 \,|\!|\!| g |\!|\!|^2_{2;\omega_z^*} + \varepsilon \,\|g\|_{2;\omega_z^*} |\!|\!| g |\!|\!|_{2;\omega_z^*}$, while $\lambda_z'^{-1} \simeq 1 + \varepsilon H_z^{-1}$ yields $\theta_z^\psi \lesssim \varepsilon^2 \,|\!|\!| g |\!|\!|^2_{2;\omega_z^\psi} + (1 + \varepsilon^2 H_z^{-2}) \|g\|^2_{2;\omega_z^\psi}$. Combining these two observations with (7), (19) and Remark 4.1 yields $\sum_{z \in \mathscr{N}} (\theta_z + \theta_z^\psi) \lesssim \Theta$.

Next, combining (27)–(30) with the above definitions of θ_z and θ_z^ψ, one gets

$$\begin{aligned} \min\big\{ |I_z + I_z^\psi|, |I_z| \big\} &\lesssim (\theta_z \lambda_z)^{1/2} \|\varepsilon J\|_{\infty;\gamma_z} \,, \\ |I_z^\psi| &\lesssim (\theta_z^\psi \lambda'_z \varepsilon H_z)^{1/2} \mathrm{osc}(\varepsilon\psi; [\gamma_z \backslash \mathring{\gamma}_z] \cap \Gamma_N). \end{aligned}$$

Now, an application of Hölder's inequality shows that $\sum_{z \in \mathscr{N}} \min\big\{ |I_z + I_z^\psi|, |I_z| \big\}$ is bounded by the right-hand side of (20), and $\sum_{z \in \mathscr{N}} |I_z^\psi|$ is bounded by the right-hand side of (21).

Finally, set $\widetilde{I}_z^\psi := 0$ if $\min\big\{ |I_z + I_z^\psi|, |I_z| \big\} = |I_z|$, and $\widetilde{I}_z^\psi := I_z^\psi$ otherwise, so that one always has $|I_z + \widetilde{I}_z^\psi| = \min\big\{ |I_z + I_z^\psi|, |I_z| \big\}$. The desired assertions (20) and (21) follow with $I^\psi := \sum_{z \in \mathscr{N}} \widetilde{I}_z^\psi$.

Hence, it remains to establish (27), (28) and (29). The bounds for I'_z and I''_z in (27), as well as I_z in (28), can be found in [9, Section 5.2, see (5.12), (5.13)]; they are obtained from (25) and (24) using (8) and (9) respectively. It should be noted that, compared to [9], there is an additional term in I'_z, which involves $\int_{\mathring{\gamma}_z \cap \Gamma^N}$ and can be easily estimated again using (8).

The proof of $I_z''' + (I_z^N + I_z^\psi) = 0$ in (27) is more delicate. It is convenient to adapt the convention that $u_h = 0$ in $\mathbb{R}^2\backslash\bar\Omega$ when computing $[\![\partial_y u_h]\!]$ across the boundary edges. With this convention, one can show, for each $z = (x_i, y_z)$, that

$$I_z''' + (I_z^N + I_z^\psi) = \varepsilon^2 \Big(\sum_{S\in\gamma_z\backslash\mathring\gamma_z} [\![\partial_y u_h]\!] \Big) \int_{x_{i-1}}^{x_i} [g(x,y_z) - \bar g_z]\, \varphi_i(x)\, dx, \tag{31}$$

with $\int_{x_{i-1}}^{x_i}$, in the case of $i = 0$, replaced by $-\int_{x_i}^{x_{i+1}}$ (see [8, 9] for similar representations of I_z'''). First, consider the case $[\gamma_z\backslash\mathring\gamma_z] \cap \Gamma^N = \varnothing$. Then $I_z''' + (I_z^N + I_z^\psi) = I_z'''$, while in the definition of I_z''', one has $\nu_y = 0$ on $\mathring\gamma_z$ and $\phi_z = \varphi_i(x)$ on $\gamma_z\backslash\mathring\gamma_z$. In the latter case, we integrate the function $[g(x,y_z) - \bar g_z]\phi_z = [g(x,y_z) - \bar g_z]\varphi_i(x)$ of one variable x, which appears in the definition (16) of $\bar g_z$. Furthermore, $\nu_y ds = dx$ on any edge connecting z to the vertical line $\{x = x_{i-1}\}$ and $\nu_y ds = -dx$ on any edge connecting z to the vertical line $\{x = x_{i+1}\}$. Rewriting the integrals over such edges as integrals with respect to x over (x_{i-1}, x_i) and (x_i, x_{i+1}), respectively, and then employing (16) for the integrals over (x_i, x_{i+1}), one arrives at (31) for the case $[\gamma_z\backslash\mathring\gamma_z] \cap \Gamma^N = \varnothing$.

If $[\gamma_z\backslash\mathring\gamma_z] \cap \Gamma^N \neq \varnothing$, we additionally need to consider the integrals in $I_z^N + I_z^\psi$ (see (26)) of the same function $[g(x,y_z) - \bar g_z]\phi_z = [g(x,y_z) - \bar g_z]\varphi_i(x)$ over the edges in $[\gamma_z\backslash\mathring\gamma_z] \cap \Gamma^N$. Note that in these integrals, $ds = dx$, while $\partial_y u_h = [\![\partial_y u_h]\!]$ on any edge in $[\gamma_z\backslash\mathring\gamma_z] \cap \Gamma^N$ connecting z to the vertical line $\{x = x_{i-1}\}$, and $\partial_y u_h = -[\![\partial_y u_h]\!]$ on any edge in $[\gamma_z\backslash\mathring\gamma_z] \cap \Gamma^N$ connecting z to the vertical line $\{x = x_{i+1}\}$. For the latter, we again employ (16) so that all integrals in $I_z^N + I_z^\psi$ are rewritten as integrals over (x_{i-1}, x_i) with respect to x. This again yields (31). So this relation is proved.

Whenever $i = n$ in (31), one immediately gets $I_z''' + (I_z^N + I_z^\psi) = 0$ from (16). Otherwise, if $0 \leqslant i \leqslant n-1$ and $y_z > 0$, noting that $[\![\partial_y u_h]\!] = 0$ on $\mathring\gamma_z$, as well as on any element edge lying on $\{x = 0\}$, one gets $\sum_{S\in\gamma_z\backslash\mathring\gamma_z} [\![\partial_y u_h]\!] = \sum_{S\in\mathscr{S}_z} [\![\partial_y u_h]\!] = 0$, so again $I_z''' + (I_z^N + I_z^\psi) = 0$ immediately follows from (16). Finally, if $y_z = 0$, one employs $g(x,y_z) = \bar g_z = 0$.

We now proceed to getting (29). Note that in the definition of I_z^ψ in (26) one has $\phi_z = \varphi_i(x)$ and $\int_{[\gamma_z\backslash\mathring\gamma_z]\cap\Gamma^N} = \int_{x_{i-1}}^{x_{i+1}} dx$. Now, if $z = (x_i, 1)$ for $1 \leqslant i \leqslant n$, recalling (16), one can replace ψ in I_z^ψ by $\psi - \psi(z)$, so

$$|I_z^\psi| \lesssim \varepsilon \left\{ \int_{[\gamma_z\backslash\mathring\gamma_z]\cap\Gamma^N} |g| \right\} \operatorname{osc}(\varepsilon\psi; [\gamma_z\backslash\mathring\gamma_z] \cap \Gamma_N).$$

This yields (29) by an application of (9), in which ω_z is replaced by any isotropic domain ω_z^ψ of type (30), and hence h_z in (9) is also replaced by H_z. The remaining case of $z = (0,1)$ is considered similarly, only using $\bar g_z = 0$ and $|\psi| \leqslant \operatorname{osc}(\varepsilon\psi; [\gamma_z\backslash\mathring\gamma_z] \cap \Gamma_N)$ (the latter follows from the final condition in (14)). This completes the proof of (27), (28) and (29), and hence of (20) and (21). □

Remark 4.5. The above proof remains valid if $\{\bar g_z\}_{z\in\mathcal{N}}$ defined by (16) are replaced by $\{\bar g_z^*\}_{z\in\mathcal{N}}$ from (17). Indeed, I_z will include an additional component $I_z^* := \varepsilon^2 \int_{\gamma_z} J(\bar g_z - \bar g_z^*)$, for which one easily gets $|I_z^*| \leqslant \varepsilon H_z |\bar g_z - \bar g_z^*|\, \|\varepsilon J\|_{\infty;\gamma_z}$. For $|I_z^*|$, bounds of type (27) and (28) are then obtained using (18); see [9, Remark 5.6].

5 Numerical results

We test the estimator of Theorem 4.1, using a simple version of (1) with $\Omega = (0,1)^2$, $\Gamma_N = \{(x,y) \in \partial\Omega : \ x = 0 \text{ or } y = 0\}$, and $f = u - F(x,y)$, where F is such that the unique exact solution $u = 4y(1-y)\left[\cos(\pi x/2) - (e^{-x/\varepsilon} - e^{-1/\varepsilon})/(1-e^{-x/\varepsilon})\right]$ (the latter exhibits a sharp boundary layer at $x = 0$). An example of anisotropic mesh refinement using similar estimators is given in [8, Section 7.7]. Here, we only consider one a-priori-chosen layer-adapted mesh, which is obtained by drawing diagonals from the tensor product of the Bakhvalov grid $\{\chi(\frac{i}{N})\}_{i=1}^{N}$ in the x-direction [2] and a uniform grid $\{\frac{j}{M}\}_{j=0}^{M}$ in the y-direction with $M = \frac{1}{2}N$ (see [9, Fig. 3 (right)], and also [7]). The continuous mesh-generating function $\chi(t) = t$ if $\varepsilon > \frac{1}{6}$; otherwise, $\chi(t) = 3\varepsilon \ln \frac{1}{1-2t}$ for $t \in (0, \frac{1}{2} - 3\varepsilon)$ and is linear elsewhere subject to $\chi(1) = 1$.

Theorem 4.1 and Corollary 4.2 give the error estimator $|||u_h - u|||_{\varepsilon;\Omega} \lesssim \mathscr{E}$, where $\mathscr{E} := \left\{\mathscr{E}_{(20)}^2 + \mathscr{E}_{(21)}^2 + \mathscr{E}_{(23)}^2 + \mathscr{E}_{(12)}^2\right\}^{1/2}$, with the notation $\mathscr{E}_{(\cdot)}$ for the right-hand side of $(\cdot)$ (e.g., $\mathscr{E}_{(12)} = \|f_h - f_h^I\|_{2;\Omega}$). By Corollary 4.2, all Θ-factors are set equal to 1. When computing the estimators, we replaced H_z from (4) by $\max_{T \subset \omega_z} H_T \simeq H_z$, and quantities of type $\min\{1, a\varepsilon^{-1}\}$ by their smoother analogues $\frac{a}{\varepsilon + a}$ (e.g., λ_z' was replaced by $\frac{H_z}{\varepsilon + H_z}$). We also replaced f_h and u by their quadratic Lagrange interpolants.

The effectivity indices in Table 1, computed as the ratio of the estimator $\mathscr{E}$ to the error $|||u_h - u|||_{\varepsilon;\Omega}$, do not exceed 7.17. Table 1 also displays the ratios of the new component $\mathscr{E}_{(21)}$ in the jump residual estimator to its more standard part $\mathscr{E}_{(20)}$; they remain between 0.18 and 1.76. Note also that for the experiments of Table 1, the ratio of $\left\{\mathscr{E}_{(20)}^2 + \mathscr{E}_{(21)}^2 + \mathscr{E}_{(23)}^2\right\}^{1/2}$ to the error component $\left\{\varepsilon^2 \|\nabla u_h - (\nabla u)^I\|_{2;\Omega}^2 + \|u_h - u^I\|_{2;\Omega}^2\right\}^{1/2}$ does not exceed 7.76.

For the considered ranges of ε and N, the aspect ratios of the mesh elements take values between 2 and 3.6e+8. Considering these variations, the estimator $\mathscr{E}$ performs quite well and its effictivity indices stabilize as $\varepsilon \to 0$. A more comprehensive numerical study of the proposed estimators certainly needs to be conducted, and will be presented elsewhere.

References

1. Ainsworth, M., Oden, J. T.: A posteriori error estimation in finite element analysis. Wiley-Interscience, New York (2000)
2. Bakhvalov, N. S.: On the optimization of methods for solving boundary value problems with boundary layers. Zh. Vychisl. Mat. Mat. Fis. **9**, 841–859 (1969) (in Russian)
3. Chadha, N. M., Kopteva, N.: Maximum norm a posteriori error estimate for a 3d singularly perturbed semilinear reaction-diffusion problem. Adv. Comput. Math. **35**, 33–55 (2011)
4. Demlow, A., Kopteva, N.: Maximum-norm a posteriori error estimates for singularly perturbed elliptic reaction-diffusion problems. Numer. Math. **133**, 707–742 (2016)
5. Kopteva, N.: Maximum norm error analysis of a 2d singularly perturbed semilinear reaction-diffusion problem. Math. Comp. **76**, 631–646 (2007)
6. Kopteva, N.: Maximum norm a posteriori error estimate for a 2d singularly perturbed reaction-diffusion problem. SIAM J. Numer. Anal. **46**, 1602–1618 (2008)

Table 1 Errors, estimators, their effectivity indices, and ratios of $\mathscr{E}_{(21)}$ to $\mathscr{E}_{(20)}$.

N	$\varepsilon=1$	$\varepsilon=2^{-5}$	$\varepsilon=2^{-10}$	$\varepsilon=2^{-15}$	$\varepsilon=2^{-20}$	$\varepsilon=2^{-25}$	$\varepsilon=2^{-30}$
	Errors $\|\|\|u_h-u\|\|\|_{\varepsilon;\Omega}$						
64	3.19e-2	4.99e-3	1.02e-3	6.71e-4	6.58e-4	6.57e-4	6.57e-4
128	1.60e-2	2.53e-3	4.26e-4	1.78e-4	1.64e-4	1.64e-4	1.64e-4
256	8.01e-3	1.28e-3	2.02e-4	5.36e-5	4.13e-5	4.08e-5	4.08e-5
512	4.01e-3	6.43e-4	9.96e-5	2.02e-5	1.06e-5	1.02e-5	1.02e-5
	Estimators $\mathscr{E}$						
64	1.12e-1	2.70e-2	5.95e-3	1.25e-3	6.83e-4	6.58e-4	6.57e-4
128	5.37e-2	1.26e-2	2.95e-3	5.60e-4	1.89e-4	1.64e-4	1.64e-4
256	2.62e-2	5.92e-3	1.45e-3	2.72e-4	6.27e-5	4.17e-5	4.08e-5
512	1.29e-2	2.83e-3	6.94e-4	1.35e-4	2.60e-5	1.10e-5	1.02e-5
	Effectivity Indices $\mathscr{E}/\|\|\|u_h-u\|\|\|_{\varepsilon;\Omega}$						
64	3.516	5.398	5.844	1.858	1.039	1.001	1.000
128	3.355	4.980	6.935	3.153	1.152	1.005	1.000
256	3.268	4.633	7.171	5.075	1.520	1.021	1.001
512	3.223	4.403	6.965	6.691	2.439	1.081	1.003
	Ratios $\mathscr{E}_{(21)}/\mathscr{E}_{(20)}$						
64	0.49	1.11	1.69	1.72	1.72	1.72	1.72
128	0.35	0.87	1.69	1.74	1.74	1.74	1.74
256	0.25	0.65	1.65	1.75	1.75	1.75	1.75
512	0.18	0.48	1.56	1.75	1.76	1.76	1.76

7. Kopteva, N.: Linear finite elements may be only first-order pointwise accurate on anisotropic triangulations. Math. Comp. **83**, 2061–2070 (2014)
8. Kopteva, N.: Maximum-norm a posteriori error estimates for singularly perturbed reaction-diffusion problems on anisotropic meshes. SIAM J. Numer. Anal. **53**, 2519–2544 (2015)
9. Kopteva, N.: Energy-norm a posteriori error estimates for singularly perturbed reaction-diffusion problems on anisotropic meshes. Numer. Math. (2017), published online 2 May 2017, DOI: 10.1007/s00211-017-0889-3
10. Kopteva, N.: Fully computable a posteriori error estimator using anisotropic flux equilibration on anisotropic meshes. Submitted for publication (2017) `http://www.staff.ul.ie/natalia/pubs.html`
11. Kopteva, N., O'Riordan, E.: Shishkin meshes in the numerical solution of singularly perturbed differential equations. Int. J. Numer. Anal. Model. **7**, 393–415 (2010)
12. Kunert, G.: An a posteriori residual error estimator for the finite element method on anisotropic tetrahedral meshes. Numer. Math. **86**, 471–490 (2000)
13. Kunert, G.: Robust a posteriori error estimation for a singularly perturbed reaction-diffusion equation on anisotropic tetrahedral meshes. Adv. Comput. Math. **15**, 237–259 (2001)
14. Kunert, G., Verfürth, R.: Edge residuals dominate a posteriori error estimates for linear finite element methods on anisotropic triangular and tetrahedral meshes. Numer. Math. **86**, 283–303 (2000)
15. Nochetto, R.H.: Pointwise a posteriori error estimates for monotone semi-linear equations. Lecture Notes at 2006 CNA Summer School Probabilistic and Analytical Perspectives on Contemporary PDEs (2006)
16. Roos, H.-G., Stynes, M., Tobiska, T.: Robust Numerical Methods for Singularly Perturbed Differential Equations. Springer, Berlin (2008)
17. Siebert, K. G.: An a posteriori error estimator for anisotropic refinement. Numer. Math. **73**, 373–398 (1996)
18. Verfürth, R.: Robust a posteriori error estimators for a singularly perturbed reaction-diffusion equation. Numer. Math. **78**, 479–493 (1998)